

Article

Dissolved Iron and Organic Matter in Boreal Rivers across a South–North Transect

Alisa Aleshina ¹, Maria-Anna Rusakova ², Olga Y. Drozdova ¹, Oleg S. Pokrovsky ^{3,4,*}  and Sergey A. Lapitskiy ¹

¹ Department of Geochemistry, Faculty of Geology, Lomonosov Moscow State University, 119991 Moscow, Russia; lis.aleshina@yandex.ru (A.A.); drozdova_olga@yahoo.fr (O.Y.D.); lapitskiy.sa@yandex.ru (S.A.L.)

² All-Russian Scientific-Research Institute of Mineral Resources Named after N. M. Fedorovsky, 119017 Moscow, Russia; greenkrok@yandex.ru

³ Geoscience and Environment Toulouse (GET), UMR 5563 CNRS University of Toulouse, 31400 Toulouse, France

⁴ BIO-GEO-CLIM Laboratory, National Research Tomsk State University, 634004 Tomsk, Russia

* Correspondence: oleg.pokrovsky@get.omp.eu

Abstract: Iron (Fe) is one of the main nutrients present in dissolved, suspended, and colloidal states in river water. Predicting the composition and size of dissolved Fe compounds is crucial for assessing water quality. In this study, we used a combination of physical methods (filtration), chemical techniques (ion exchange chromatography), and thermodynamic modeling (Visual MINTEQ) to characterize dissolved Fe speciation in boreal organic-rich rivers across a sizable south–north transect. We chose contrasting rivers with a predominance of either allochthonous or autochthonous organic compounds. We found that the dissolved organic matter (DOM) in the studied rivers varies in molecular weights and the degree of humification. Regardless of the climate parameters of the river watershed, the dominant status of dissolved Fe during the summer low-water period was essentially colloidal and dominated by anionic complexes of the type $[\text{MeL}]^{n-}$.

Keywords: dissolved organic matter; iron; speciation; rivers; boreal zone



Citation: Aleshina, A.; Rusakova, M.-A.; Drozdova, O.Y.; Pokrovsky, O.S.; Lapitskiy, S.A. Dissolved Iron and Organic Matter in Boreal Rivers across a South–North Transect. *Environments* **2024**, *11*, 65. <https://doi.org/10.3390/environments11040065>

Academic Editors: Xiaopeng Huang, Qian Zhao and Lanfang Han

Received: 31 January 2024

Revised: 18 March 2024

Accepted: 25 March 2024

Published: 26 March 2024



Copyright: © 2024 by the authors. Licensee MDPI, Basel, Switzerland. This article is an open access article distributed under the terms and conditions of the Creative Commons Attribution (CC BY) license (<https://creativecommons.org/licenses/by/4.0/>).

1. Introduction

It is well-known that peatlands cover only 3% of the Earth's land surface, with 80% of them located in the temperate–cold climates of the northern hemisphere, particularly in Russia, Canada, and the USA. Despite their relatively small coverage, peatlands store about 15–30% of the world's soil carbon [1]. Allochthonous organic matter emerges as a crucial factor influencing the ecosystems of water bodies in northern temperate regions [2–4], contributing to the characteristic dark coloration of peatland waters [5]. The primary factors influencing seasonal fluctuations in the color of surface waters include climate parameters, such as precipitation and temperature [6].

Over past decades, several studies have demonstrated the darkening of both lentic and lotic waters in northern regions, a phenomenon referred to as water brownification [7–9]. For instance, a distinct trend towards increased water color has been reported in Petrozavodsk Bay and the Central Onego Lake water column, accompanied by a simultaneous rise in total iron and CO₂ concentrations in the epilimnion and a decrease in pH values during summer [4]. These trends are driven by several factors, including global climate warming [5,10–13], changes in land-use (e.g., artificial ditching or forestry [6,14–16]), and decreasing acid deposition [17]. Among the climatic factors, a particular role has been attributed to increased precipitation [18] and, overall, milder winters [16,19].

It has long been recognized that the coloration of boreal humic waters is influenced not only by dissolved organic matter (DOM) but also by dissolved Fe [20–23], which is known to be organically bound, particularly to high-molecular-weight organic colloids [24–27]. Recent investigations have demonstrated an increase in the total dissolved Fe concentration

in boreal waters over past decades [20–22,28–30]. It has been shown that riverine Fe export flux is positively correlated with that of dissolved organic carbon (DOC) [23,31]. Furthermore, some studies have reported that iron contribution to the light absorption of DOM varies significantly across seasons and space [32,33].

Increased releases of DOM and Fe from terrestrial to aquatic ecosystems have profound implications for downstream water quality, affecting temperature stratification, oxygen concentration, light penetration depth, and qualitative composition of DOM, thereby influencing nutrient cycling [3,16,34,35]. Brownification can especially affect light-sensitive phytoplankton, macrophytes, and algae [36,37], altering the composition of carbon compounds in the water column [38]. Additionally, it can change the input of growth-limiting DOM-associated iron particles to aquatic ecosystems [35,39,40]. Furthermore, not only the quantity but also, to a greater extent, the qualitative characteristics of solutes, such as dissolved and particulate iron speciation, become a significant factor influencing the status of rivers and lakes [41,42]. It is known that most dissolved Fe in boreal waters is present in the form of organic and organo-mineral colloids (from 1 nm to 0.22 μm), whose transport and bioavailability are drastically differ from those of inorganic ions or simple organic complexes [43]. Therefore, the composition and size distribution of Fe-bearing compounds are crucial for evaluating the current state and predicting potential alterations in water quality under intensifying anthropogenic pressures and climate warming.

In order to improve our knowledge of the current status of surface waters in the European boreal zone and to characterize the mechanisms governing coupled iron–carbon biogeochemical processes, here we investigated 14 rivers in different regions of the European part of Russia across a sizable (1300 km) south–north transect. We chose contrasting rivers of different size, containing both allochthonous and autochthonous organic compounds. Employing a combination of size separation (filtration and ultrafiltration), chemical techniques (ion exchange chromatography), and thermodynamic modeling (Visual MINTEQ), this comprehensive approach provided new insights into the forms of iron present in the studied rivers.

2. Materials and Methods

2.1. Study Site Description

We selected a set of fourteen boreal rivers, located in different regions of the European part of Russia (Figure 1): Vologda Oblast (Ivnyashka, Koy, Kovzha, Ilexa rivers); Tver Oblast (Mezha River); Vladimir Oblast (Senga River); Leningrad Oblast (Cherpayoki, Pionerka, and Mga rivers); and the Republic of Karelia (Lundozhma, Ukhta, Olanga, Vuoksa, and Lemb rivers). Samples were collected during the summer low-water season in 2018 and 2019.



Figure 1. Map of the sampling points. The parameters of the river watersheds are listed in Table 1.

Table 1. Characteristics of the study sites.

Object Name	River Length ¹ , km	Watershed Area ¹ , km ²	MAAT ² , °C	MAP ² , mm/day ¹
Senga	32	163	3.74	1.27
Mezha	168	2630	3.66	1.55
Ivnyashka	14.3	29	2.16	1.72
Mga	93	754	3.46	1.73
Koy	14	27	1.85	1.72
Ilexa	4.7	32	1.46	1.72
Kovzha	108	1080	1.53	1.72
Pionerka	4.6	7.9	3.49	1.73
Vuoksa	143	68,700	3.21	1.73
Lemb	1.8	2.1	1.79	1.72
Lundozhma	11.1	64.2	0.97	1.73
Ukhta	47	380	0.12	1.73
Cherpayoki	13	17	0.12	1.73
Olanga	67	5679	−0.62	1.83

¹ Data from the Russian State Water Register. ² MAAT—mean annual air temperatures, MAP—mean annual precipitation, 30-year average annual values according to the <https://power.larc.nasa.gov/data-access-viewer/> (accessed on 30 January 2024).

The main physio-geographic characteristics of sampled rivers and their localization are presented in Table 1. The sample points are located along a 1300-km-long N–S transect from Moscow City to the polar circle. Moving northward, there is a general decrease in agricultural and industrial activity, as well as overall population density on the river watersheds. The NW European part of Russia is characterized by a flat relief, often marshy. From Moscow to approximately 60° N latitude, rivers drain through sedimentary rocks (carbonates, clays), while in the most northwest part, the Fennoscandian Shield dominates the watershed lithology, consisting of granites and gneisses with exposures of basic rocks, quartzites, and sandstones. However, all mother rocks are covered by glacial moraine deposits.

The sampled rivers vary significantly in length and drainage area. The largest among them is Vuoksa, which constitutes a series of lakes bound together by shorter riverlike connections across Russia and Finland (with a drainage basin at the sampling point of 68,700 km²). The other largest rivers are Olanga (5679 km²), Mezha (2630 km²), and Kovzha (1080 km²). The other rivers have drainage basin areas from 2 to 800 km², and the smallest among them is Lemb Creek with a catchment area of only 2 km². The lengths of the studied watercourses vary from 2 km (Lemb) to 168 km (Mezha).

Mean annual air temperatures (MAAT) for the study watersheds range from −0.62 °C to 3.74 °C. Significant temperature changes occur both from south to north and from east to west. For example, the difference in mean annual temperature between the Kovzha and Ivnyashka rivers, which are located at the same latitude, is 2 °C. Only the Olanga River catchment is characterized by a negative mean annual temperature (−0.62 °C). A much smaller gradient is observed for the mean annual precipitation (MAP), which gradually increases from 464 in the south to 668 mm y^{−1} in the north.

2.2. Chemical Analyses

In the field, pH and Electrical Conductivity (E.C.) were measured using the “Hanna HI 9033” conductivity meter and the “Hanna HI 9025” pH meter (Hanna Instruments, Lingo Tanneries, France). The water temperature at the time of sample collection did not vary more than 4–5 °C among different rivers (Table S1 in Supplementary Materials). Water samples were collected near the middle of the flow at a depth of 10–15 cm in 1-L high-density polyethylene (HDPE) containers without headspace. Immediately after sampling, the waters were filtered through a sterilized 0.22 µm Lavsan filter (FiTreM[®], INNIT), removing particles and a portion of bacteria [44–46]. For major cation and Fe analyses by ICP-MS, the filtered samples were collected into acid-cleaned polypropylene 15 mL vials and acidified with bidistilled HNO₃. For the measurement of dissolved organic carbon,

anions, and optical spectra, no acidification was performed on the samples in the 20 mL glass vials. Prior to laboratory analysis, the water samples were kept at 4 °C for less than three days.

The determination of colloidal and truly dissolved fractions was carried out via a conventional size fractionation procedure. Sample fractionation was achieved through filtration using acetate-cellulose filters with different pore sizes (Millipore). The separation of suspended and dissolved forms (the sum of colloidal and truly dissolved) was performed using membrane filters with a pore diameter of 0.22 µm, employing syringe attachments. The separation of colloidal forms from truly dissolved forms was accomplished through ultrafiltration with a pore size of 1 kDa, using a 50 mL polycarbonate cell (Amicon 8050) equipped with a suspended magnetic stirrer positioned a few millimeters above the filter to prevent pore clogging during filtration. Details of size separation procedure and discussion of relevant yields and artefacts are provided in former works of our group [47,48].

The experimental determination of the content of anionic metal compounds in the dissolved fraction was performed using ion-exchange chromatography with an anion-exchange resin DEAE-cellulose (Sigma Aldrich, St. Louis, MO, USA). The sample was passed through glass columns filled with cellulose ionite in Cl-form (at a flow rate of ~1 cm³/min). The column dimensions were 90 mm in length, 25 mm in diameter, and the height of the sorbent was 40 mm. The sum of cationic and neutral forms of metals was determined in the eluate. The experiment was performed in triplicate for each sample.

Optical (UV and visual range) spectra of the samples were recorded using the 511 UV/Vis spectrophotometer (Portlab, Moscow, Russia) in the wavelength range of 200–700 nm with a resolution of 1 nm. The values of the E₂₅₄/E₄₃₆ and E₄₇₀/E₆₅₅ ratios, spectral slopes (S_{275–295}; S_{350–400}), slope ratio (S_R), and specific UV absorbance (SUVA₂₅₄) were calculated according to standard methods [47,49].

In the laboratory, the samples were analyzed for inorganic anion content using an ion chromatograph “Dionex ICS2000”, Thermo Fisher Scientific (Waltham, MA, USA), and dissolved organic carbon (DOC) was determined using the “LiquiTOC trace” analyzer, Elementar (Langensfeld, Germany). Alkalinity was measured by potentiometric titration with HCl to pH = 4.2 using a Gran method (pH meter “Hanna HI 9025”, Hanna Instruments, Lingo Tanneries, France). Major cations and Fe content in the samples were determined using ICP-MS Elan 6100 DRC (Perkin Elmer, Waltham, MA, USA) and Agilent 5000 (Agilent Technologies, Santa Clara, CA, USA), the uncertainty of element concentration measurements ranged from 5 to 10% at [C] > 1 µg/L. The international geostandard SLRS-4 was used to verify the reproducibility of the results.

Based on all the obtained hydrochemical characteristics, calculations of Fe forms in the studied water bodies were performed using the Visual MINTEQ program ver. 3.1 [50]. The input parameters were pH, concentrations of major cations, anions, DOC and metal content of the initial solution. The Stockholm Humic Model (SHM) for metal complexation with organic matter was employed in the calculations [50]. Unlike the NICA–Donnan model, the SHM model relies on a set of empirically derived relationships and a certain number of binding sites with varying affinities in order to calculate metal speciation. In other words, DOM sites can be assumed to have a discrete set of pK_a values. This is in many ways similar to Models V/VI/VII [51–53], but it utilizes the Stern model to take into account electrostatic interactions [50]. At the present time, there is insufficient data to compare these models to judge which one is more accurate.

In this study, all DOM (including both the proton- and metal-binding fractions) was assumed to be comprised of fulvic acid with a carbon content of 50%. To characterize proton and metal binding, we utilized generic parameters for fulvic acid [54]. The equilibrium constants were derived from the NIST database [55]. The output data are the concentration of each species bound to organic and inorganic ligands. Further details of major and trace metal speciation calculations in boreal humic waters are provided elsewhere [46].

The data were tested for normality using the Shapiro–Wilk test. Mean and standard deviation values (mean ± standard deviation) were used to assess the uncertainty in the

data from the three replicate measurements. Correlations were tested using the Spearman correlation coefficient (R), with *p*-values less than 0.05 considered significant. All graphs were created using MS Excel 2021.

3. Results and Discussion

3.1. Main Physical and Hydrochemical Characteristics

The pH values in studied water bodies ranged from neutral (6.9) to slightly alkaline (8.0) (Table 2). Electrical conductivity (κ) varied between 26–307 $\mu\text{S}/\text{cm}$. The DOC concentration ranged from 6 to 27 mg/L, which is typical for boreal rivers draining peatland and taiga areas [39,56,57]. The Fe content did not exceed 1 mg/L in any sample and the maximum iron content was found in the Cherpayoki River (0.94 mg/L). Considering all the water samples studied, there was no correlation between Fe and DOC concentrations ($R^2 = 0.09$ for the linear regression).

Table 2. The main chemical characteristics of the research objects (<0.22 μm filtrates).

River	pH	κ	HCO_3^-	Cl^-	NO_3^-	SO_4^{2-}	Na	Mg	K	Ca	DOC	Fe
		$\mu\text{S}/\text{cm}$	mg/L									
Senga	7.6	94	122.9	5.1	2.8	4.8	2.0	3.9	0.7	23.0	22	0.19
Mezha	7.6	36	35.3	1.2	1.1	0.6	1.0	1.8	0.4	11.7	19	0.37
Ivnyashka	7.3	78	51	7.9	4.8	3.3	5.0	3.9	1.6	11.9	22	0.13
Mga	7.8	244	202	15.1	0.9	12.4	8.6	12.7	3.0	49.0	8	0.17
Koy	7.8	214	176.2	0.6	n.d.	1.5	2.6	10.5	1.4	35.5	20	0.05
Ilexa	8.0	307	44.5	110.9	1.2	3.5	1.7	17.8	1.1	46.8	6	0.15
Kovzha	7.9	26	0.4	2.3	n.d.	18.1	0.8	1.3	0.5	3.9	13	0.19
Pionerka	7.5	54	0.5	31.0	1.9	3.9	4.0	2.5	1.8	6.3	7	0.02
Vuoksa	7.5	57	35.2	3.3	2.3	4.6	3.7	2.7	1.9	6.7	15	0.03
Lemb	7.8	33	31.7	0.6	0.2	1.0	1.5	1.4	0.5	16.6	22	0.43
Lundozhma	7.1	39	36.7	3.9	0.3	0.7	4.5	2.4	0.4	14.9	27	0.57
Ukhta	7.7	27	18.9	0.4	0.1	0.6	1.4	1.5	0.5	2.5	8	0.15
Cherpayoki	6.9	33	42.2	23.7	0.1	0.4	4.0	2.1	25.5	3.2	12	0.94
Olanga	7.5	47	31.2	0.7	0.8	1.9	1.2	1.9	0.9	6.6	6	0.03

The waters of the examined rivers are predominantly fresh and ultra-fresh, belonging to the hydrocarbonate class with calcium and magnesium–calcium dominance and a lesser presence of sodium (Table 2). However, the waters of the Kovzha River fall into the sulfate class, whereas the waters of the Ilexa, Pionerka, and Cherpayoki rivers belong to the chloride class. No correlation was found between the parameters described in Table 2 and the geographical characteristics of the sampled water bodies, including latitude, catchment area, watercourse length, MAAT, and MAP (Table S2).

In Russia, in accordance with SanPiN 1.2.3685-21, the permissible limit of iron concentration in waters of fisheries reservoirs is 0.1 mg/L. For waters used for household, drinking, and cultural purposes, the concentration of iron must not exceed 0.3 mg/L, which is consistent with the recommendations of the World Health Organization. The concentrations of Fe in the studied rivers were generally below the maximum allowable concentration set by Russian legislation, with the exception of the Mezha, Lundozhma, Lemb, and Cherpayoki rivers.

3.2. Characterization of Dissolved Organic Matter

The spectral DOM characteristics allowed qualitative comparison of the studied river-water samples (Table 3). The SUVA_{254} values below four indicated that autochthonous DOM predominated in the Pionerka, Lemb, Ilexa, Vuoksa, Ukhta, and Olanga rivers, while allochthonous DOM dominated in the Mezha and Senga rivers (4.2 and 4.9, respectively).

Table 3. Spectral characteristics of the investigated water samples.

Object Name	E_{254}/E_{436}	E_{470}/E_{655}	$S_{275-295}$	$S_{350-400}$	S_R	$SUVA_{254}$
Senga	20.0	10.3	0.016	0.019	0.84	4.9
Mezha	15.8	8.3	0.014	0.017	0.84	4.2
Ivnyashka	9.2	3.3	0.013	0.013	0.97	2.7
Mga	22.5	4.0	0.017	0.019	0.89	2.7
Koy	19.7	20.0	0.016	0.018	0.92	3.3
Ilexa	34.8	3.0	0.019	0.02	0.93	2.3
Kovzha	19.3	7.5	0.015	0.018	0.85	3.3
Pionerka	22.0	2.0	0.019	0.015	1.21	1.8
Vuoksa	11.9	2.8	0.015	0.015	0.98	2.5
Lemb	14.3	20.0	0.013	0.016	0.80	2.1
Lundozhma	12.6	11.8	0.013	0.016	0.81	3.3
Ukhta	49.5	3.0	0.019	0.023	0.83	2.5
Cherpayoki	14.2	9.5	0.013	0.017	0.73	3.6
Olanga	20.1	5.0	0.015	0.018	0.84	3.0

The lowest values of the E_{470}/E_{655} ratio were observed in the waters of the Vuoksa and Pionerka rivers, which reflects the largest molecular size of DOM in these rivers. The lowest values of the E_{254}/E_{436} ratios were recorded for the Ivnyashka, Vuoksa, and Lundozhma rivers, while higher values (>30) were characteristic for the Ilexa and Ukhta rivers, indicating a higher degree of humification of organic matter in those waters compared to other samples.

The rivers Cherpayoki, Lundozhma, Ivnyashka, and Lemb exhibited the lowest spectral slope ($S_{275-295}$), while the rivers Pionerka, Ilexa, and Ukhta demonstrated the highest. River Ivnyashka had the lowest spectral slope ($S_{350-400}$), while the rivers Ilexa and Ukhta had the largest. The lower slope coefficient values suggest that the content of the colloidal DOM pool in these rivers is higher. The slope ratio (S_R), which correlates with the distribution of molecular masses of DOM, was highest in the rivers Ivnyashka, Vuoksa, and Pionerka, and lowest in the Cherpayoki River.

The relationship between mean latitude of the river watershed and the main optical characteristics are shown in Figure S1. No significant correlation with latitude was found for any of the coefficients. The same was true about the relationship of MAAT with the studied optical characteristics (Figure S2). It is possible that optical properties of DOM are closely linked to the site and type of DOM. In fact, in the catchment area of some rivers, there are numerous wetlands, which could be the major contributor to the DOM concentration of these objects.

3.3. Forms of Iron Presence in the Studied Water Bodies

The concentration of dissolved iron varies from 0.02 to 0.94 mg/L (Table 2). The elevated Fe content in the waters of the Mezha, Lundozhma, and Cherpayoki rivers (0.37, 0.57 and 0.94 mg/L, respectively) could be attributed to the wetland-dominated terrain through which these rivers flow.

The concentrations of Fe in most of the studied rivers (with the exceptions of the Pionerka, Vuoksa, and Olanga rivers) are consistent with those reported for the Russian Arctic Rivers in the White Sea (0.06–0.59 mg/L), Pechora Sea (0.3 mg/L), Kara Sea (0.07–0.57 mg/L), Laptev Sea (0.08 mg/L), and East Siberian Sea (0.05 mg/L) watersheds [58]. These findings are also generally consistent with the average concentration of dissolved Fe in rivers worldwide (66 mkg/L) [59].

The results of ultrafiltration showed that the predominant dissolved form of iron is colloids of 1 kDa to 0.22 μ m (Figure 2). Only in the Pionerka and Olanga rivers did iron predominate in the truly dissolved (low molecular weight) form. These rivers are characterized by the lowest DOC and iron contents.

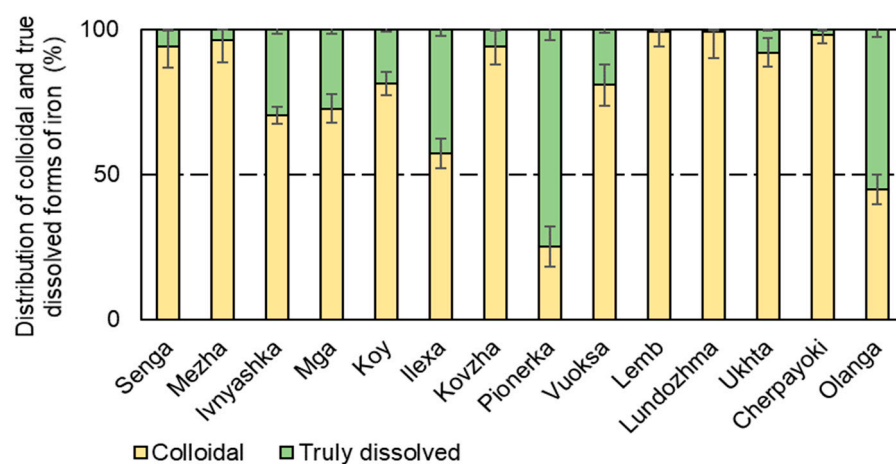


Figure 2. Distribution of colloidal (1 kDa–0.22 μm) and true dissolved (<1 kDa) forms of iron in studied rivers of NW Europe (see locations in Figure 1).

No significant correlation was found between the percentage of colloidal Fe and latitude, MAAT, and MAP of sample points (Figure S3).

Thermodynamic modeling using the Visual MINTEQ program demonstrated that Fe is predominantly present in the form of complexes with organic matter in almost all studied water bodies (Figure 3, Table S3). Not more than 3% of the total dissolved Fe content was represented by inorganic compounds in the Mga, Ilexa, and Cherpayoki water samples.

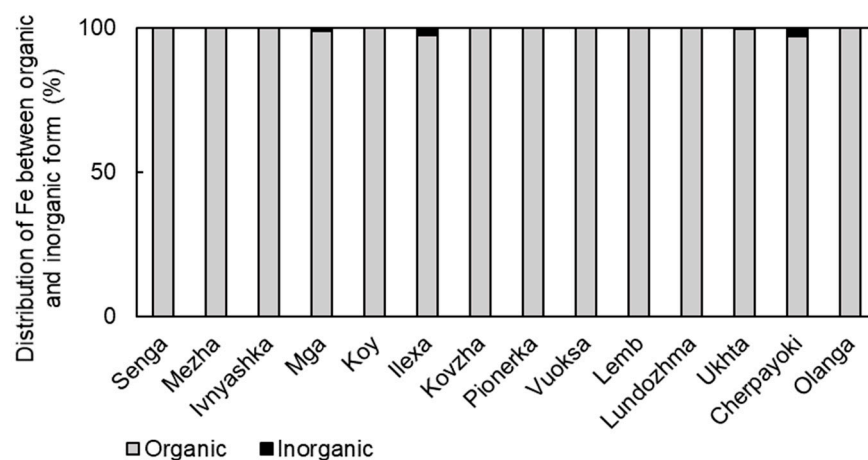


Figure 3. Distribution of iron forms between organic and inorganic forms according to Visual MINTEQ modeling. Organic complexes of metals include both low-molecular-weight organic ligands and organic colloids, such as fulvic acid.

The obtained ion exchange chromatography data indicated that for Fe, anionic complexes of the form $[\text{MeL}]^{n-}$ predominated (Figure 4). Given that thermodynamic calculations (Figure 3) predict that a majority of dissolved Fe is associated with organic compounds, these complexes are likely formed by high-molecular-weight organic matter as it is known in the temperate humic waters [60]. However, in the Mga, Ilexa, Pionerka, Vuoksa, and Olanga rivers, a significant portion of Fe was present in cationic or neutral complexes of the form $[\text{MeL}]^{n+}$ and $[\text{MeL}]^0$, respectively. It is likely that such complexes are formed with low-molecular-weight organic ligands, including products of the metabolism of aquatic microorganisms. This correlates with the low SUVA_{254} values in these samples (from 1.8 to 3.0), emphasizing the predominance of autochthonous organic matter and its association with iron, respectively.

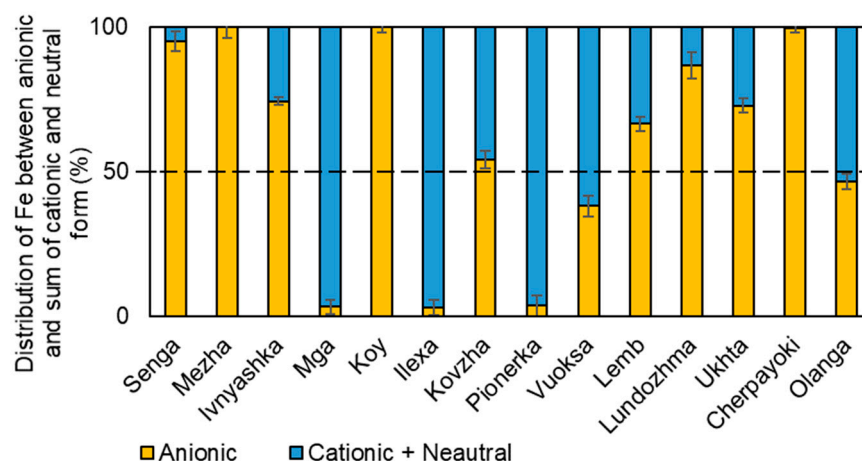


Figure 4. The proportion of anionic $[\text{MeL}]^{n-}$ and the sum of cationic $[\text{MeL}]^{n+}$ and neutral $[\text{MeL}]^0$ forms of iron in the studied waters.

There was no correlation between such characteristics as latitude, river length, fraction of low-molecular-weight iron, and the fraction of iron in anionic form in water samples (Figure S4). No significant correlation was found between the percentage of anionic Fe and pH (Figure S5). At the same time, there was a correlation between some optical characteristics (SUVA_{254} , E_{470}/E_{655} , $S_{275-295}$ and S_R) and the percentage of anionic Fe. Such positive correlations could be indicative of the dominance of aromatic molecules in the anionic Fe complexes.

3.4. Comparison with Results of Previous Studies of Boreal River Waters

It is interesting to compare the results of the present study with those obtained about 20 years ago for other rivers across a similar, 1500-km long, south–north transect of NW European Russia [39]. Figure 5 shows the distribution of pH values, DOC, Fe_{diss} ($<0.22 \mu\text{m}$ filtrates), and $\text{Fe}_{<1 \text{ kDa}}$ concentrations in river samples collected in 1999–2000 by Pokrovsky and Schott [39] and the present work (2018–2019). Median and mean values of pH and DOC were slightly higher for water samples taken in 1999–2000 than samples taken in 2018–2019. The Fe_{diss} and $\text{Fe}_{<1 \text{ kDa}}$ concentrations, on the other hand, were found to be higher in the previously collected samples. We hypothesize that variations in pH, DOC, and iron content can be attributed to differences in climatic conditions during the sampling years (precipitation and temperature). These parameters may, in turn, influence (1) the degree of river water fed by surrounding bogs, providing high-molecular-weight aromatic OM, (2) connectivity to the groundwater, which provides the input of Fe(II) necessary for the formation of organo-ferric colloids in the riparian/hyporheic zone, and (3) in-stream aquatic primary productivity, providing autochthonous, low-molecular-weight organic ligands. The complexity and simultaneous operation of these often counteracting factors could explain why there was no correlation between the contents of Fe_{diss} , $\text{Fe}_{<1 \text{ kDa}}$, and pH value and the geographical location (latitude) of the sampled water bodies.

There was less data available to compare the proportions of colloidal iron relative to the total dissolved form assessed in summers 1999 and 2000 [39]. The values obtained in the two studies are equally independent of the latitude, and no specific patterns are observed in their distribution (Figure 6). The fundamental significance of this result is that there is no straightforward control of river size and climatic parameters on Fe speciation, its interaction with DOM, and the size fraction of colloids. We therefore suggest that the main controlling factors of DOM and Fe abundance in river water are the number of wetlands in the watershed and the degree of connectivity between Fe(II)-rich underground waters and the river waters [61]. The latter occurs via local discharge within the riparian or hyporheic zone of the stream, so that ionic Fe(II), which is present in the partially anoxic groundwater, is subjected to oxidation and stabilization in the form of organo-ferric colloids in the

oxygenated water column of the river [39]. This potentially allows for the approximation of the main features of Fe-DOM interaction across the boreal regions, although the local features of the watershed (wetland, riparian zone, groundwater connectivity, water column, periphyton productivity, and respiration) could lead to strong variability in the proportion of colloidal Fe within relatively short geographical distances.

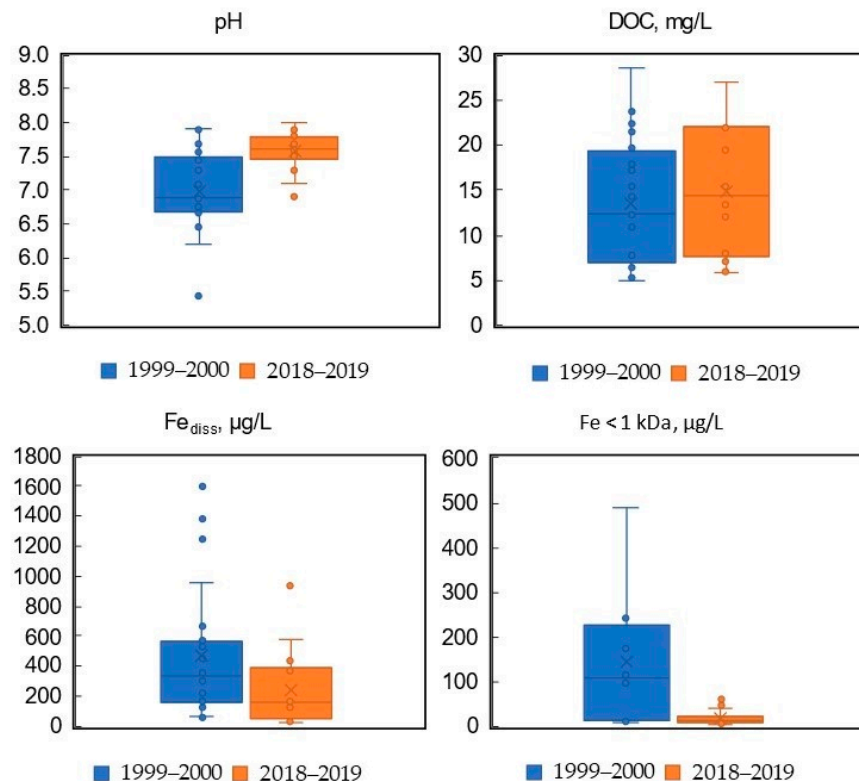


Figure 5. Distribution of pH values, DOC, and Fe concentrations in the <0.22 µm filtrates and Fe in the <1 kDa filtrates of river samples of the present study (2018–2019) and those given by Pokrovsky and Schott (1999–2000) [39].

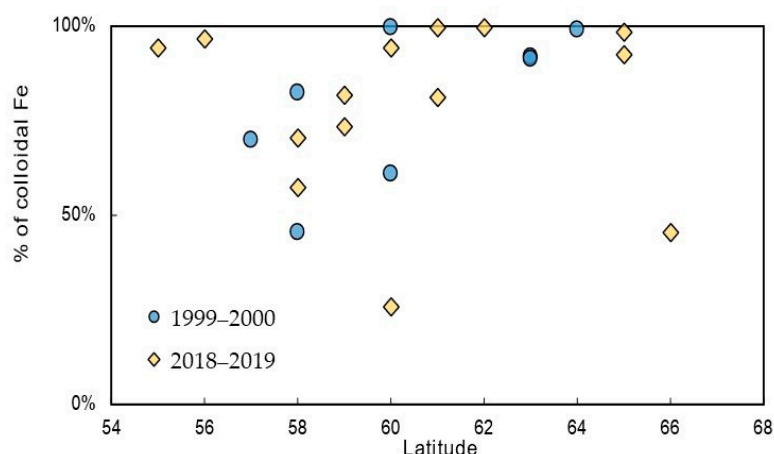


Figure 6. Distribution of % colloidal (1 kDa–0.22 µm) Fe as a function of latitude in rivers of NW European Russia sampled in the present study (2018–2019) and those given by Pokrovsky and Schott (1999–2000) [39].

4. Conclusions

Boreal rivers of the European part of Russia exhibited a high concentration of dissolved Fe and DOC. Analysis of 14 rivers across a sizable climate gradient showed that there is

no correlation between the concentration of these components, pH value, content of main cations and anions, and geographical position (latitude) of the river sampling point.

Analysis of UV-visual spectral data revealed that allochthonous organic compounds dominate in the Mezha and Senga rivers, which have abundant peatlands at their watersheds, while autochthonous compounds likely prevailed in other rivers. Differences in the qualitative characteristics of the organic matter of the studied rivers could be related to pH values, as the Ivnyashka, Pionerka, Vuoksa, and Lundozhma rivers are characterized by the lowest pH values among the selected samples. Note, however, that we did not evidence any correlation between the percentage of colloidal Fe and the pH of the river water.

In the studied rivers, the Fe concentrations were generally below the maximum allowed concentration established by the Russian legislation, except for the Mezha, Lundozhma, Lemb, and Cherpayoki rivers. This is attributed to the physiogeographical conditions of the territories (wetlands, bogs and fens) through which these rivers flow. The concentrations of dissolved Fe in the rivers studied are generally consistent with values in the global river runoff.

In all river waters sampled over the 1300 km south–north transect, dissolved iron was almost entirely represented by compounds with organic ligands. During the summer low-water period, the predominant form of dissolved Fe in the investigated waters was colloidal (1 kDa–0.22 μm) anionic complexes $[\text{MeL}]^{n-}$. The only exceptions were samples from the Pionerka and Olanga rivers, which are characterized simultaneously by the lowest total dissolved Fe and DOC concentration. We argue that, given the lack of relationship between the chemical/colloidal status of both Fe and DOM, and the morphological (watershed size and river length) and climatic parameters of the river watershed, the main features of the Fe-DOM interaction revealed in the present study could be potentially extrapolated to the entire boreal region of Northern Eurasia.

Supplementary Materials: The following supporting information can be downloaded at: <https://www.mdpi.com/article/10.3390/environments11040065/s1>. Table S1: Water temperature values at the time of sampling; Table S2: Coefficients of determination (R^2) of the main chemical characteristics (<0.22 μm filtrates) and physiographic characteristics of the research objects; Table S3: The iron species in the studied waters (%) as calculated by vMINTEQ.; Figure S1: No correlations of main optical characteristics with latitude of sample points.; Figure S2: Lack of correlations between main optical characteristics with mean annual air temperature (MAAT, $^{\circ}\text{C}$) of sample points.; Figure S3: Lack of correlations between the percentage of colloidal Fe and latitude, mean annual air temperature (MAAT, $^{\circ}\text{C}$) and mean annual precipitation (MAP, mm/day) of samples river watersheds.; Figure S4: Lack of correlations between the percentage of anionic Fe and latitude, river length (km) and % of LMW_{<1kDa} Fe.; Figure S5: Lack of correlations between the percentage of anionic Fe vs. pH and most optical characteristics.

Author Contributions: Conceptualization, O.S.P. and A.A.; methodology, S.A.L. and O.Y.D.; validation, O.S.P.; formal analysis, O.S.P. and A.A.; investigation, M.-A.R., A.A. and O.Y.D.; data curation, M.-A.R., A.A. and S.A.L.; writing—original draft preparation, O.S.P. and A.A.; visualization, A.A.; funding acquisition, O.Y.D. All authors have read and agreed to the published version of the manuscript.

Funding: This research was funded by the RSF, grant number 21-77-10028 (analysis and interpretation). O.P. was partially funded by the TSU Development Programme Priority-2030.

Data Availability Statement: The data presented in this study are available on request from the corresponding author. The data are not publicly available due to their intended use for the development of technology and equipment.

Conflicts of Interest: The authors declare no conflicts of interest.

References

1. Limpens, J.; Berendse, F.; Blodau, C.; Canadell, J.G.; Freeman, C.; Holden, J.; Roulet, N.; Rydin, H.; Schaepman-Strub, G. Peatlands and the Carbon Cycle: From Local Processes to Global Implications—A Synthesis. *Biogeosciences* **2008**, *5*, 1475–1491. [[CrossRef](#)]
2. Williamson, C.E.; Morris, D.P.; Pace, M.L.; Olson, O.G. Dissolved Organic Carbon and Nutrients as Regulators of Lake Ecosystems: Resurrection of a More Integrated Paradigm. *Limnol. Oceanogr.* **1999**, *44*, 795–803. [[CrossRef](#)]
3. Solomon, C.T.; Jones, S.E.; Weidel, B.C.; Buffam, I.; Fork, M.L.; Karlsson, J.; Larsen, S.; Lennon, J.T.; Read, J.S.; Sadro, S.; et al. Ecosystem Consequences of Changing Inputs of Terrestrial Dissolved Organic Matter to Lakes: Current Knowledge and Future Challenges. *Ecosystems* **2015**, *18*, 376–389. [[CrossRef](#)]
4. Kalinkina, N.; Tekanova, E.; Korosov, A.; Zobkov, M.; Ryzhakov, A. What Is the Extent of Water Brownification in Lake Onego, Russia? *J. Great Lakes Res.* **2020**, *46*, 850–861. [[CrossRef](#)]
5. George, G. *The Impact of Climate Change on European Lakes*; Springer: Berlin/Heidelberg, Germany, 2010; ISBN 978-90-481-2944-7.
6. Klante, C.; Larson, M.; Persson, K.M. Brownification in Lake Bolmen, Sweden, and Its Relationship to Natural and Human-Induced Changes. *J. Hydrol. Reg. Stud.* **2021**, *36*, 100863. [[CrossRef](#)]
7. Zhu, X.; Chen, L.; Pumpanen, J.; Keinänen, M.; Laudon, H.; Ojala, A.; Palviainen, M.; Kiirikki, M.; Neitola, K.; Berninger, F. Assessment of a Portable UV-Vis Spectrophotometer's Performance for Stream Water DOC and Fe Content Monitoring in Remote Areas. *Talanta* **2021**, *224*, 121919. [[CrossRef](#)] [[PubMed](#)]
8. Hongve, D.; Riise, G.; Kristiansen, J.F. Increased Colour and Organic Acid Concentrations in Norwegian Forest Lakes and Drinking Water—A Result of Increased Precipitation? *Aquat. Sci.* **2004**, *66*, 231–238. [[CrossRef](#)]
9. Weyhenmeyer, G.A.; Karlsson, J. Nonlinear Response of Dissolved Organic Carbon Concentrations in Boreal Lakes to Increasing Temperatures. *Limnol. Oceanogr.* **2009**, *54*, 2513–2519. [[CrossRef](#)]
10. Eikebrokk, B.; Vogt, R.D.; Liltved, H. NOM Increase in Northern European Source Waters: Discussion of Possible Causes and Impacts on Coagulation/Contact Filtration Processes. *Water Supply* **2004**, *4*, 47–54. [[CrossRef](#)]
11. Erlandsson, M.; Buffam, I.; Fölster, J.; Laudon, H.; Temnerud, J.; Weyhenmeyer, G.A.; Bishop, K. Thirty-Five Years of Synchrony in the Organic Matter Concentrations of Swedish Rivers Explained by Variation in Flow and Sulphate. *Glob. Chang. Biol.* **2008**, *14*, 1191–1198. [[CrossRef](#)]
12. *Finland's Sixth National Communication under the United Nations Framework Convention on Climate Change*; Ministry of the Environment and Statistics Finland: Helsinki, Finland, 2013; p. 314.
13. *Assessment Report on Climate Change and Its Consequences in Russian Federation*; Federal Service for Hydrometeorology and Environmental Monitoring: Moscow, Russia, 2008; p. 54.
14. Worrall, F.; Harriman, R.; Evans, C.D.; Watts, C.D.; Adamson, J.; Neal, C.; Tipping, E.; Burt, T.; Grieve, I.; Monteith, D.; et al. Trends in Dissolved Organic Carbon in UK Rivers and Lakes. *Biogeochemistry* **2004**, *70*, 369–402. [[CrossRef](#)]
15. Estlander, S.; Pippingsköld, E.; Horppila, J. Artificial Ditching of Catchments and Brownification-Connected Water Quality Parameters of Lakes. *Water Res.* **2021**, *205*, 117674. [[CrossRef](#)] [[PubMed](#)]
16. Horppila, J.; Nurminen, L.; Rajala, S.; Estlander, S. Making Waves: The Sensitivity of Lakes to Brownification and Issues of Concern in Ecological Status Assessment. *Water Res.* **2024**, *249*, 120964. [[CrossRef](#)] [[PubMed](#)]
17. Asmala, E.; Carstensen, J.; Räike, A. Multiple Anthropogenic Drivers behind Upward Trends in Organic Carbon Concentrations in Boreal Rivers. *Environ. Res. Lett.* **2019**, *14*, 124018. [[CrossRef](#)]
18. Ledesma, J.L.J.; Futter, M.N.; Laudon, H.; Evans, C.D.; Köhler, S.J. Boreal Forest Riparian Zones Regulate Stream Sulfate and Dissolved Organic Carbon. *Sci. Total Environ.* **2016**, *560–561*, 110–122. [[CrossRef](#)] [[PubMed](#)]
19. de Wit, H.A.; Valinia, S.; Weyhenmeyer, G.A.; Futter, M.N.; Kortelainen, P.; Austnes, K.; Hessen, D.O.; Räike, A.; Laudon, H.; Vuorenmaa, J. Current Browning of Surface Waters Will Be Further Promoted by Wetter Climate. *Environ. Sci. Technol. Lett.* **2016**, *3*, 430–435. [[CrossRef](#)]
20. Kritzberg, E.S.; Ekström, S.M. Increasing Iron Concentrations in Surface Waters – a Factor behind Brownification? *Biogeosciences* **2012**, *9*, 1465–1478. [[CrossRef](#)]
21. Sarkkola, S.; Nieminen, M.; Koivusalo, H.; Laurén, A.; Kortelainen, P.; Mattsson, T.; Palviainen, M.; Piirainen, S.; Starr, M.; Finér, L. Iron Concentrations Are Increasing in Surface Waters from Forested Headwater Catchments in Eastern Finland. *Sci. Total Environ.* **2013**, *463–464*, 683–689. [[CrossRef](#)] [[PubMed](#)]
22. Xiao, Y.-H.; Hoikkala, L.; Kasurinen, V.; Tirola, M.; Kortelainen, P.; Vähätalo, A.V. The Effect of Iron on the Biodegradation of Natural Dissolved Organic Matter. *J. Geophys. Res. Biogeosci.* **2016**, *121*, 2544–2561. [[CrossRef](#)]
23. Heikkinen, K.; Saari, M.; Heino, J.; Ronkanen, A.-K.; Kortelainen, P.; Joensuu, S.; Vilmi, A.; Karjalainen, S.-M.; Hellsten, S.; Visuri, M.; et al. Iron in Boreal River Catchments: Biogeochemical, Ecological and Management Implications. *Sci. Total Environ.* **2022**, *805*, 150256. [[CrossRef](#)]
24. Shapiro, J. The Relation of Humic Color to Iron in Natural Waters. *Int. Ver. Für Theor. Und Angew. Limnol. Verhandlungen* **1966**, *16*, 477–484. [[CrossRef](#)]
25. Hunter, K.A.; Boyd, P.W. Iron-Binding Ligands and Their Role in the Ocean Biogeochemistry of Iron. *Environ. Chem.* **2007**, *4*, 221–232. [[CrossRef](#)]
26. Gledhill, M.; Buck, K. The Organic Complexation of Iron in the Marine Environment: A Review. *Front. Microbiol.* **2012**, *3*, 18807. [[CrossRef](#)]

27. Drozdova, O.Y.; Aleshina, A.R.; Tikhonov, V.V.; Lapitskiy, S.A.; Pokrovsky, O.S. Coagulation of Organo-Mineral Colloids and Formation of Low Molecular Weight Organic and Metal Complexes in Boreal Humic River Water under UV-Irradiation. *Chemosphere* **2020**, *250*, 126216. [[CrossRef](#)] [[PubMed](#)]
28. Ekström, S.M.; Regnell, O.; Reader, H.E.; Nilsson, P.A.; Löfgren, S.; Kritzberg, E.S. Increasing Concentrations of Iron in Surface Waters as a Consequence of Reducing Conditions in the Catchment Area. *J. Geophys. Res. Biogeosci.* **2016**, *121*, 479–493. [[CrossRef](#)]
29. Björnerås, C.; Weyhenmeyer, G.A.; Evans, C.D.; Gessner, M.O.; Grossart, H.-P.; Kangur, K.; Kokorite, I.; Kortelainen, P.; Laudon, H.; Lehtoranta, J.; et al. Widespread Increases in Iron Concentration in European and North American Freshwaters. *Glob. Biogeochem. Cycles* **2017**, *31*, 1488–1500. [[CrossRef](#)]
30. Guan, J.; Qi, K.; Wang, J.; Zhuang, J.; Yuan, X.; Yan, B.; Lu, N.; Qu, J. Effects of Conversion from Boreal Natural Wetlands to Rice Paddy Fields on the Dynamics of Total Dissolved Iron during Extreme Precipitation Events. *Chemosphere* **2020**, *242*, 125153. [[CrossRef](#)] [[PubMed](#)]
31. Knorr, K.-H. DOC-Dynamics in a Small Headwater Catchment as Driven by Redox Fluctuations and Hydrological Flow Paths—Are DOC Exports Mediated by Iron Reduction/Oxidation Cycles? *Biogeosciences* **2013**, *10*, 891–904. [[CrossRef](#)]
32. Brezonik, P.L.; Finlay, J.C.; Griffin, C.G.; Arnold, W.A.; Boardman, E.H.; Germolus, N.; Hozalski, R.M.; Olmanson, L.G. Iron Influence on Dissolved Color in Lakes of the Upper Great Lakes States. *PLoS ONE* **2019**, *14*, e0211979. [[CrossRef](#)]
33. Xiao, Y.; Riise, G. Coupling between Increased Lake Color and Iron in Boreal Lakes. *Sci. Total Environ.* **2021**, *767*, 145104. [[CrossRef](#)] [[PubMed](#)]
34. Ejankowski, W.; Lenard, T. Climate Driven Changes in the Submerged Macrophyte and Phytoplankton Community in a Hard Water Lake. *Limnologia* **2015**, *52*, 59–66. [[CrossRef](#)]
35. Cuss, C.W.; Ghotbizadeh, M.; Grant-Weaver, I.; Javed, M.B.; Noernberg, T.; Shoty, W. Delayed Mixing of Iron-Laden Tributaries in Large Boreal Rivers: Implications for Iron Transport, Water Quality and Monitoring. *J. Hydrol.* **2021**, *597*, 125747. [[CrossRef](#)]
36. Creed, I.F.; Bergström, A.-K.; Trick, C.G.; Grimm, N.B.; Hessen, D.O.; Karlsson, J.; Kidd, K.A.; Kritzberg, E.; McKnight, D.M.; Freeman, E.C.; et al. Global Change-Driven Effects on Dissolved Organic Matter Composition: Implications for Food Webs of Northern Lakes. *Glob. Chang. Biol.* **2018**, *24*, 3692–3714. [[CrossRef](#)] [[PubMed](#)]
37. Choudhury, M.I.; Urrutia-Cordero, P.; Zhang, H.; Ekvall, M.K.; Medeiros, L.R.; Hansson, L.-A. Charophytes Collapse beyond a Critical Warming and Brownification Threshold in Shallow Lake Systems. *Sci. Total Environ.* **2019**, *661*, 148–154. [[CrossRef](#)] [[PubMed](#)]
38. Zheng, L.; Xing, Y.; Ding, A.; Sun, S.; Cheng, H.; Bian, Z.; Yang, K.; Wang, S.; Zhu, G. Brownification of Freshwater Promotes Nitrogen-Cycling Microorganism Growth Following Terrestrial Material Increase and Ultraviolet Radiation Reduction. *Sci. Total Environ.* **2022**, *853*, 158556. [[CrossRef](#)] [[PubMed](#)]
39. Pokrovsky, O.S.; Schott, J. Iron Colloids/Organic Matter Associated Transport of Major and Trace Elements in Small Boreal Rivers and Their Estuaries (NW Russia). *Chem. Geol.* **2002**, *190*, 141–179. [[CrossRef](#)]
40. Trick, C.G.; Bill, B.D.; Cochlan, W.P.; Wells, M.L.; Trainer, V.L.; Pickell, L.D. Iron Enrichment Stimulates Toxic Diatom Production in High-Nitrate, Low-Chlorophyll Areas. *Proc. Natl. Acad. Sci. USA* **2010**, *107*, 5887–5892. [[CrossRef](#)] [[PubMed](#)]
41. Hassellöv, M.; von der Kammer, F. Iron Oxides as Geochemical Nanovectors for Metal Transport in Soil-River Systems. *Elements* **2007**, *4*, 401. [[CrossRef](#)]
42. Saari, M.; Rossi, P.M.; Postila, H.; Marttila, H. Predicting Iron Transport in Boreal Agriculture-Dominated Catchments under a Changing Climate. *Sci. Total Environ.* **2020**, *714*, 136743. [[CrossRef](#)] [[PubMed](#)]
43. Oleinikova, O.V.; Poitrasson, F.; Drozdova, O.Y.; Shirokova, L.S.; Lapitskiy, S.A.; Pokrovsky, O.S. Iron Isotope Fractionation during Bio- and Photodegradation of Organoferric Colloids in Boreal Humic Waters. *Environ. Sci. Technol.* **2019**, *53*, 11183–11194. [[CrossRef](#)] [[PubMed](#)]
44. Hahn, M.W. Broad Diversity of Viable Bacteria in “sterile” (0.2 Microm) Filtered Water. *Res. Microbiol.* **2004**, *155*, 688–691. [[CrossRef](#)] [[PubMed](#)]
45. Liu, J.; Li, B.; Wang, Y.; Zhang, G.; Jiang, X.; Li, X. Passage and Community Changes of Filterable Bacteria during Microfiltration of a Surface Water Supply. *Environ. Int.* **2019**, *131*, 104998. [[CrossRef](#)] [[PubMed](#)]
46. Nakai, R. Size Matters: Ultra-Small and Filterable Microorganisms in the Environment. *Microbes Environ.* **2020**, *35*, ME20025. [[CrossRef](#)] [[PubMed](#)]
47. Ilina, S.M.; Drozdova, O.Y.; Lapitskiy, S.A.; Alekhin, Y.V.; Demin, V.V.; Zavgorodnyaya, Y.A.; Shirokova, L.S.; Viers, J.; Pokrovsky, O.S. Size Fractionation and Optical Properties of Dissolved Organic Matter in the Continuum Soil Solution-Bog-River and Terminal Lake of a Boreal Watershed. *Org. Geochem.* **2014**, *66*, 14–24. [[CrossRef](#)]
48. Ilina, S.M.; Lapitskiy, S.A.; Alekhin, Y.V.; Viers, J.; Benedetti, M.; Pokrovsky, O.S. Speciation, Size Fractionation and Transport of Trace Elements in the Continuum Soil Water–Mire–Humic Lake–River–Large Oligotrophic Lake of a Subarctic Watershed. *Aquat. Geochem.* **2016**, *22*, 65–95. [[CrossRef](#)]
49. Peacock, M.; Evans, C.D.; Fenner, N.; Freeman, C.; Gough, R.; Jones, T.G.; Lebron, I. UV-Visible Absorbance Spectroscopy as a Proxy for Peatland Dissolved Organic Carbon (DOC) Quantity and Quality: Considerations on Wavelength and Absorbance Degradation. *Environ. Sci. Process. Impacts* **2014**, *16*, 1445–1461. [[CrossRef](#)]
50. Gustafsson, J.P. Visual MINTEQ Ver. 3.1. 2014. Available online: <http://vminteq.lwr.kth.se> (accessed on 15 February 2020).
51. Tipping, E.; Hurley, M.A. A Unifying Model of Cation Binding by Humic Substances. *Geochim. Cosmochim. Acta* **1992**, *56*, 3627–3641. [[CrossRef](#)]

52. Tipping, E.; Lofts, S.; Sonke, J. Humic Ion-Binding Model VII: A Revised Parameterisation of Cation-Binding by Humic Substances. *Environ. Chem.* **2011**, *8*, 225. [CrossRef]
53. Lofts, S.; Tipping, E. Assessing WHAM/Model VII against Field Measurements of Free Metal Ion Concentrations: Model Performance and the Role of Uncertainty in Parameters and Inputs. *Environ. Chem.* **2011**, *8*, 501–516. [CrossRef]
54. Gustafsson, J.P.; Kleja, D.B. Modeling Salt-Dependent Proton Binding by Organic Soils with the NICA-Donnan and Stockholm Humic Models. *Environ. Sci. Technol.* **2005**, *39*, 5372–5377. [CrossRef] [PubMed]
55. Burgess, D. NIST SRD 46. Critically Selected Stability Constants of Metal Complexes: Version 8.0 for Windows, National Institute of Standards and Technology 2004. Available online: <https://doi.org/10.18434/M32154> (accessed on 20 December 2023).
56. Selberg, A.; Viik, M.; Ehapalu, K.; Tenno, T. Content and Composition of Natural Organic Matter in Water of Lake Pitkjärv and Mire Feeding Kuke River (Estonia). *J. Hydrol.* **2011**, *400*, 274–280. [CrossRef]
57. Xue, J.-P.; Cuss, C.W.; Noernberg, T.; Javed, M.B.; Chen, N.; Pelletier, R.; Wang, Y.; Shotyk, W. Size and Optical Properties of Dissolved Organic Matter in Large Boreal Rivers during Mixing: Implications for Carbon Transport and Source Discrimination. *J. Hydrol. Reg. Stud.* **2022**, *40*, 101033. [CrossRef]
58. Savenko, A.V.; Savenko, V.S. Trace Element Composition of the Dissolved Matter Runoff of the Russian Arctic Rivers. *Water* **2024**, *16*, 565. [CrossRef]
59. Gaillardet, J.; Viers, J.; Dupré, B. Trace Elements in River Waters. *Treatise Geochem.* **2004**, *5*, 225–272.
60. Drozdova, O.Y.; Karpukhin, M.M.; Dumtsev, S.V.; Lapitskiy, S.A. The Forms of Metals in the Water and Bottom Sediments of the Malaya Sen'ga River (Vladimir Oblast). *Mosc. Univ. Geol. Bull.* **2021**, *76*, 336–342. [CrossRef]
61. Krickov, I.V.; Pokrovsky, O.S.; Manasypov, R.M.; Lim, A.G.; Shirokova, L.S.; Viers, J. Colloidal Transport of Carbon and Metals by Western Siberian Rivers during Different Seasons across a Permafrost Gradient. *Geochim. Cosmochim. Acta* **2019**, *265*, 221–241. [CrossRef]

Disclaimer/Publisher's Note: The statements, opinions and data contained in all publications are solely those of the individual author(s) and contributor(s) and not of MDPI and/or the editor(s). MDPI and/or the editor(s) disclaim responsibility for any injury to people or property resulting from any ideas, methods, instructions or products referred to in the content.